

**Accepted Manuscript**

Material requirements for magnetic refrigeration applications

Behzad Monfared

DOI: [10.1016/j.ijrefrig.2018.08.012](https://doi.org/10.1016/j.ijrefrig.2018.08.012)

Reference: IJIR 4079

To appear in: International Journal of Refrigeration

Received date: 23 March 2018

Accepted date: 19 August 2018

Available online: 4 September 2018

# Material requirements for magnetic refrigeration applications

Behzad Monfared<sup>a,\*</sup>, Björn Palm<sup>a</sup>

<sup>a</sup> KTH Royal Institute of Technology, School of Industrial Engineering and Management, Department of Energy Technology, Brinellvägen 68, SE-100 44 Stockholm, Sweden

\* Corresponding author. Tel.: +46 8 790 81 54; fax.: +46 8 20 41 61.

E-mail address: [behzadam@kth.se](mailto:behzadam@kth.se) (Behzad Monfared)

Accepted Manuscript

## Abstract

A primary motivation underlying the research on room-temperature magnetic refrigeration is reaching energy efficiency levels beyond what is achievable with vapor-compression technology. However, the goal of building commercially viable magnetic refrigeration systems with high performance and competitive price has not been achieved yet. One of the obstacles to reach this goal is the inadequate properties of the currently existing magnetocaloric materials. In this article, the needed improvements in the properties of the magnetocaloric materials is investigated. Two existing vapor-compression refrigerators are used as reference for the required performance, and magnetic refrigerators are simulated using a numerical model. Apart from the requirements such as uniformity of transition temperature for each layer, small increment in transition temperature in adjacent layers, and mechanical strength of the materials, the study shows that for the investigated cases materials with adiabatic entropy change 2.35 times larger than the existing materials are needed to outperform vapor-compression systems.

**Keywords:** Magnetocaloric, Material, Magnetic, Refrigeration, Cooling.

### Nomenclature:

$a$	specific surface area, ratio of surface area of particles to volume of bed ( $\text{m}^{-1}$ )
$a_1$	field-dependent parameter in Eq. 16 ( $\text{J kg}^{-1} \text{K}^{-1}$ )
$a_2$	field-dependent parameter in Eq. 16 ( $\text{J kg}^{-1} \text{K}^{-1}$ )
$A_c$	cross section area of packed bed ( $\text{m}^2$ )
$b_1$	field-dependent parameter in Eq. 16 (K)
$b_2$	field-dependent parameter in Eq. 16 (K)
$c_1$	field-dependent parameter in Eq. 16 (K)
$c_2$	field-dependent parameter in Eq. 16 (K)
$c_H$	heat capacity at constant magnetic field and pressure ( $\text{J kg}^{-1} \text{K}^{-1}$ )
$c_P$	heat capacity at pressure ( $\text{J kg}^{-1} \text{K}^{-1}$ )
$COP$	coefficient of performance (dimensionless)
$d_p$	particle diameter (m)
$Ex_Q$	exergetic cooling power (W)
$FWHM_s$	full width at half-maximum of $\Delta S_m - T$ curve (K)
$H$	magnetic field strength ( $\text{A m}^{-1}$ )
$h$	convective heat transfer coefficient ( $\text{W m}^{-2} \text{K}^{-1}$ )
$i$	specific enthalpy ( $\text{J kg}^{-1}$ )
$k$	thermal conductivity ( $\text{W m}^{-1} \text{K}^{-1}$ )
$L$	length of the regenerator (m)
$M$	magnetization ( $\text{A m}^{-1}$ )

$\dot{m}$	mass flow rate ( $\text{kg s}^{-1}$ )
$N$	demagnetizing factor of a packed bed of particles (dimensionless)
$Nr$	number of regenerators
$P$	power (W) or ( $\text{kWh (24h)}^{-1}$ )
$P$	pressure (Pa)
$p_0, p_1, p_2$	coefficients of polynomial Eqs. 17 and 18
$Pr$	Prandtl number (dimensionless)
$Q_C$	cooling capacity or total cooling load (W)
$Q_H$	heating capacity or rate of rejected heat (W)
$R^2$	coefficient of determination, showing closeness of data to fitted line
$RCP_s$	relative cooling power ( $\text{J kg}^{-1}$ )
$Re_d$	Reynolds, $\rho_f V_D d_p / \mu_f$ (dimensionless)
$s$	entropy ( $\text{J kg}^{-1} \text{K}^{-1}$ )
$T$	temperature (K)
$t$	time (s)
$UA$	product of overall heat transfer coefficient and heat transfer surface area ( $\text{W K}^{-1}$ )
$V_{air}$	volumetric flow rate of air $\text{m}^3 \text{s}^{-1}$
$V_D$	superficial velocity ( $\text{m s}^{-1}$ )
$\dot{W}$	mechanical power (W)
$x$	position along regenerator (m)

#### Greek symbols

$\Delta s_m$	absolute value of isentropic entropy change (magnetocaloric effect) ( $\text{J kg}^{-1} \text{K}^{-1}$ )
$\Delta T_{ad}$	adiabatic temperature change (magnetocaloric effect) (K)
$\varepsilon$	porosity (void fraction) of packed bed (dimensionless)
$\epsilon$	effectiveness (of heat exchanger) (dimensionless)
$\eta$	efficiency (dimensionless)
$\mu$	dynamic viscosity (Pa s)
$\rho$	density ( $\text{kg m}^{-3}$ )
$\tau$	cycle period (s)

#### Subscripts

C	cold reservoir
cond	condenser
corr	corrected
ef	effective
evap	evaporator
ex	external
f	fluid
H	warm reservoir
in	internal
L	fluid leaving the regenerator
m	magnetic
max	maximum
R	fluid returning from heat exchanger
s	solid
sf	solid-fluid interface

#### Abbreviations

CHX	cold heat exchanger (of magnetic refrigeration system)
EEI	energy efficiency index
HHX	hot heat exchanger (of magnetic refrigeration system)
HTF	heat transfer fluid
mat	material
MCE	magnetocaloric effect
MCM	magnetocaloric material(s)
NTU	number of transfer units (dimensionless)

## 1 Introduction

The research work on magnetic refrigeration with room-temperature applications has increased significantly since Brown (1976) proved the possibility of producing significant cooling power and temperature lift using a continuous magnetic refrigeration cycle working near room-temperature. The main drives for the research in this field have been elimination of the gaseous refrigerants leaking into the ambient and reaching higher energy efficiency. In addition to these two, other aspects such as cost, environmental impacts, weight, compactness, and reliability are also important in the path of commercialization of this technology.

Regarding the works done on improving the performance of the room-temperature magnetic refrigeration systems, the numerous built prototypes are reviewed by Balli et al. (2017) and Kitanovski et al. (2015) and efforts on modeling such systems are reviewed by Nielsen et al. (2011). The currently existing magnetocaloric materials used for room-temperature magnetic refrigeration are reviewed by Balli et al. (2017), Brück et al. (2008), Franco et al. (2012), and Gutfleisch et al. (2011).

As some researchers have mentioned, the magnetocaloric materials (MCM) for room temperature magnetic refrigeration applications need to be improved further, so that magnetic refrigeration can compete with vapor-compression technology (Bjørk et al. 2016, Dung et al. 2011, Lei et al. 2017, Tura and Rowe 2011). This study is done as a response, as requested by one of the pioneering companies active in materials sector, to the question “how much do the magnetocaloric materials need to be improved so that magnetic refrigeration can compete with vapor-compression in terms of performance?” This is a broad question which can be interpreted variously and our response is formulated through the assumptions and considerations explained in this article.

Niknia et al. (2017) have reviewed the metrics for ranking the magnetocaloric materials. In their study, active magnetic regenerators with one layer of magnetocaloric materials are modeled and the operating parameters are optimized to maximize exergetic cooling power for each of the material used as refrigerant. Then, the metrics are correlated with the maximum energetic cooling power obtained from each single-layer regenerator. Despite the lower isothermal entropy change in materials going through second order phase transition, they are ranked higher than materials showing first order phase transition because of the wider curves of their magnetocaloric effect (MCE) versus temperature. However, in applications with considerable temperature difference between the cold and warm reservoirs, a number of layers of magnetocaloric materials with different transition temperatures are used to compensate for the narrow width of the magnetocaloric effect. Therefore, Niknia et al. (2017) have differentiated between metrics suitable for single-layered regenerators and metrics for multi-layered regenerators.

In this study performance of magnetic refrigerators with multi-layered regenerators is compared with the performance of vapor-compression refrigerators working at the same conditions. In the cases that the currently existing magnetocaloric materials are not adequate to have the same or better cooling capacity and efficiency, it is investigated how much the properties of MCM should be improved. However, it should be noted that the suggested improvements in the material properties do not substantiate the claim that such materials with improved properties are necessarily possible to make. There are many potential, room-temperature applications for magnetic refrigeration with different working temperatures (temperature spans) and cooling or heating capacities. Among different applications two refrigerators, one with rather high cooling capacity and low efficiency, case 1, and another one with low cooling capacity and high efficiency, case 2, are chosen for this study. The specifications of the vapor-compression version of these two refrigerators are provided by Electrolux AB. The evaluation of the performance of the vapor-compression refrigerators is done by Electrolux AB according to the standards EN-153- 2006 and IEC-62552-2007. It implies that the given cooling loads are essentially the heat leakage to the refrigerated compartment without food inside and door openings during steady state cycling. In case of the display cabinet, the power of lighting inside the cabinet is added to the cooling load. The tool used to evaluate the performance of the magnetic refrigerators is a numerical simulation model of active magnetic regeneration, validated and presented in details by Monfared (2018a) with some modifications explained in section 2.4.

## 2 Method

In this section, the assumptions, the simulation model and optimization process, the method of modeling magnetocaloric materials and altering their properties, and the two cases for which the performance of the

existing vapor-compression systems (cooling capacity and  $COP_{total}$ ) is compared with the simulated magnetic refrigeration systems are presented. What is meant by  $COP_{total}$  is the cooling capacity divided by the total electric power input to the system.

## 2.1 Material requirements which are assumed unfulfilled

Although a disadvantage with packed beds as regenerators is their high pressure drop, which increases both pumping power consumption and viscous dissipation loss, most of the best performing built magnetic refrigeration prototypes use them as regenerators since they are more practical (Monfared 2018a, Lei et al. 2017). The reasons that alternative geometries such as parallel plates or minichannels cannot easily replace the packed beds are: the low thermal conductivity of the magnetocaloric materials necessitating very thin structures for the regenerators to facilitate heat transfer from the inner parts of the material to their surfaces; low mechanical strength and manufacturability of the promising magnetocaloric materials for making thin structures; manufacturing precision lower than the required tolerance in creating the regenerators' geometry (Lei et al. 2017, Nielsen et al. 2014, Tušek et al. 2014).

In this study, it is not assumed that all these problems are solved and the focus is still on packed beds as regenerators.

## 2.2 Material requirements which are assumed fulfilled

With increased number of layers of MCM, the transition temperatures of the magnetocaloric materials, about which the magnetocaloric effect is maximum, match the working temperatures better. With higher number of layers the increment between the transition temperatures of the consecutive layers should decrease. The decrease in the increment of the transition temperature from layer to layer is, however, limited by the difficulties in manufacturing magnetocaloric materials. For example, the layers of  $\text{La}(\text{Fe},\text{Mn},\text{Si})_{13}\text{H}_z$  supplied by one of the main manufacturers of MCM are minimum 2 K different in their nominal transient temperature. However, with some manual separation techniques it is possible to get 1 K increment in the transition temperature of the consecutive layers (Monfared and Palm 2016). Assuming that a similar separation method can be automated, the 1 K increment in the transition temperature of the consecutive layers is considered in this study. Although smaller increments can increase the cooling capacity, the gain is not considerable after a certain number of layers (Lei et al. 2015, Monfared 2018a). In addition, it is assumed that each layer of the magnetocaloric materials is not thinner than 1 mm and the particles are spherical with uniform size.

A problem with some of the magnetocaloric materials, as supplied by the manufacturers, is the spread in their transition temperature. That is, the particles supplied for each layer do not have exactly the same transition temperature (the nominal transition temperature for that layer), but the transition temperature is distributed over a range (Monfared and Palm 2016, Neves Bez et al. 2016, Radulov et al. 2015). Methods such as separation of the particles similar to the process explained by Monfared and Palm (2016) resolves, at least to some extent, this problem. In this study it is assumed that this problem is solved and within each layer all the particles have the same transition temperature.

Another shortcoming of some of the currently existing materials, such as  $\text{La}(\text{Fe},\text{Mn},\text{Si})_{13}\text{H}_z$ , is their low mechanical strength and pulverization in magnetic refrigeration cycle. The practical solution for this problem is bonding particles by an epoxy structure; nevertheless, the epoxy reduces the performance by increasing the pressure drop and hindering heat transfer from the solid particles to the heat transfer fluid (HTF) as discussed by Monfared (2018a). In this study it is assumed that the problem of mechanical stability of the materials is solved and no binding agent is needed.

Furthermore, it is assumed that the magnetocaloric materials show negligibly small hysteresis.

### 2.3 Assumptions about the rest of the system

To get the best design for different parts of the magnetocaloric refrigeration systems (optimum design of the magnetic circuit, geometry of the regenerators, layers, flow distribution system, and the heat exchangers) is one of the ultimate goals of the magnetic refrigeration community. Since this hypothetical, best design is not known to us for the time being, we cannot base this study on that. In addition, there would be different best designs depending on the parameters for which the system was optimized. Another difficulty with working with such hypothetical best design would be that the whole system should be redesigned and optimized for every individual simulation for the parametric studies done in this work, which is not practical. For example, it is not practical to redesign and optimize the magnetic circuit each time the aspect ratio of the regenerators changes in the simulations or to redesign the heat exchangers for each flow rate. Therefore, to conduct this study, the actual, detailed design of the system is not considered and the study is simplified by making well-described, reasonable assumptions.

A difficulty with choosing the magnitude and temporal variations of the magnetic field is that this choice changes the answer to the question asked by the industrial partner. For example if huge magnets, regardless of their cost and environmental impacts, are used to create a large magnetic field, lower requirements for the magnetocaloric materials are needed to compete with vapor-compression systems. This difficulty is resolved by choosing a magnet design using magnet materials sparingly and estimating the magnetic field based on such a design. The reason for this choice is that, although economic and environmental aspects are not directly mentioned in the question by the industrial partner, the high cost and environmental impacts of magnet materials make designs with large amount of magnets (creating large fields) impractical.

Another aspect, although not emphasized in the question by the industrial partner but meaningful to consider, is the physical size of the magnetic refrigeration system. In principle, when cooling capacity of a unit is not enough, it can be scaled up or multiple units can be used in parallel; however, in practice usually the available space is not unlimited. The magnetic refrigeration prototype at KTH Royal Institute of Technology, described by Monfared (2018a), is originally designed to occupy the same space that the vapor-compression system considered in case 1 does. Therefore, considering its rather compact design, the total volume of the regenerators in the prototype is used as the basis for the maximum allowed volume of the regenerators in this study. The volume of the magnetocaloric materials (together with the maximum strength of the magnetic field) indirectly affect the volume of the magnet material as well. The reason is that the amount of magnet material should be enough to create the desired field in the volume occupied by the magnetocaloric materials.

The chosen upper limit for the total volume of the regenerators (altogether), determining the amount of MCM used, is  $360 \text{ cm}^3$ . This regenerator volume is equal to that of the prototype reported by Jacobs et al. (2014), one of the best performing prototypes reported in the open literature with large cooling capacity, and is almost equal to the regenerator volume of the prototype at KTH (Monfared 2018a). The number of regenerators among which the total amount of magnetocaloric material is distributed is assumed four with two magnet poles. However, this assumption does not affect the results as long as the number of magnet poles and regenerators vary proportionally so that the pattern for magnetic field change shown in Figure 1 is maintained. If, for example, the number of regenerators are doubled, their cross section area is halved to keep the same total volume of the regenerators. Then with halved flow rate of HTF in each regenerator, the velocity, which is flow rate divided by cross section area, is the same, and therefore, the simulation model gives the same output.

The assumed pattern for the change of magnetic field and flow rate over time is shown in Figure 1. With thicker regenerators the demagnetizing factor reduces which is in favor of having larger internal magnetic field. However, to create the magnetic field in thicker regenerators more magnet material per unit length is

needed. To avoid such complications, implying designing the magnetic circuit for each single simulation, which are not the main interest of this work, the same internal field is assumed for all the simulations. In addition, the conversion from the external, applied magnetic field to the effective, internal field requires the knowledge of the demagnetizing factor, which depends on the actual shape of the regenerators, whereas the actual shape of the regenerators is not designed in this study for each single simulation as explained before. The magnitude of the internal field is chosen based on the KTH prototype which has a compact design, using magnet material sparingly, as described by Monfared (2018a). The assumption of the same internal field means that the amount of magnet needed in practice is not necessarily exactly the same for different simulations.

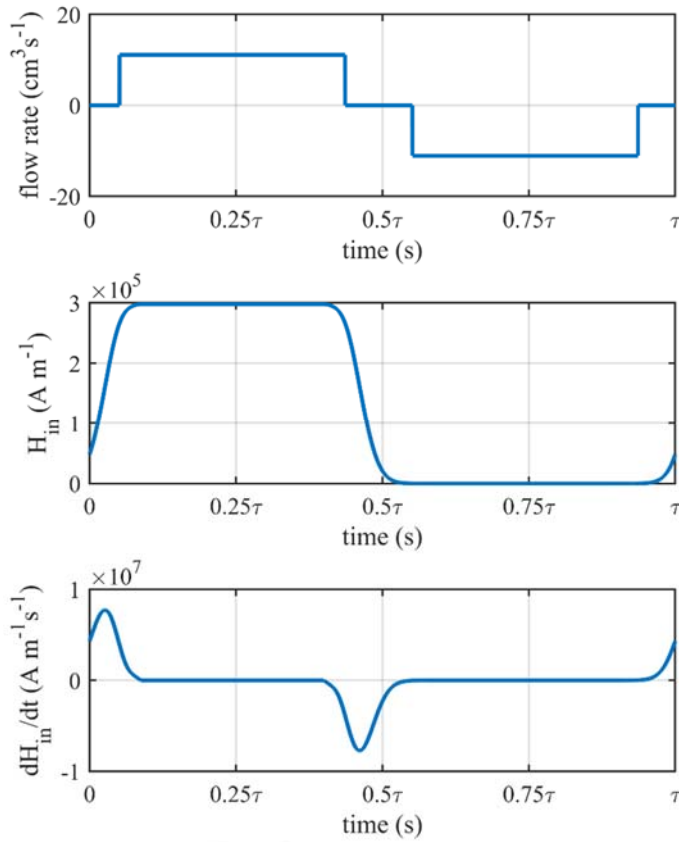


Figure 1: Assumed variation in magnetic field and flow during one cycle. The maximum flow rate can be different in the simulations.

Initially, only for calculating parasitic heat transfer as heat flux to the regenerators, it was assumed that the perimeter of the bed varies according to  $\frac{Perimeter}{61} = \sqrt{\frac{Area}{207}}$ . That is, only for parasitic heat transfer the shape of the regenerators used in KTH prototype (with perimeter of 61 mm and cross section area of 207 mm<sup>2</sup>) was preserved, but it was scaled. The correlations used for estimating the parasitic heat transfer to the regenerator were derived using a similar method explained by Monfared (2018a). Since the exact final design of the modeled systems in each simulation is not known it was a rough estimation. However, since the estimated parasitic heat transfer was negligible compared to the cooling load of the simulated cases, it is ignored in the final simulations presented here.

It is assumed that the fan energy consumption of the heat exchangers of the magnetic refrigeration systems during 24 hours are equal to those of the corresponding vapor-compression refrigerators with which they are compared. However, unlike the actual vapor-compression systems, which have on-off control, it is assumed that the magnetic refrigeration systems work continuously; therefore, the fan power is lower to have the same energy consumption during 24 hours of operation. The air flow rate over the heat exchangers of the magnetic refrigerators is adjusted using Eq. 1 according to the affinity laws. The assumption that the heat transfer coefficient on the air-side dominates the UA-values of the heat exchangers (as the heat transfer on the liquid side is considerably higher) and the assumption that the flow is turbulent on the air-side give Eq. 2. Combining Eq. 1 and Eq. 2 results in Eq. 3, by which  $UA$  is estimated for magnetic refrigerators.

$$V_{air} \propto P_{fan}^{1/3} \quad (1)$$

$$UA \propto V_{air}^{0.8} \quad (2)$$

$$UA \propto P_{fan}^{0.8/3} \quad (3)$$

The assumption that the equivalent magnetic refrigerators work continuously while the actual vapor-compression systems have on-off cycles favors the magnetic refrigeration systems since the cycling losses are avoided. However, this assumption is made to make the simulations simpler and doable in reasonable time.

The highest operation frequency considered for the simulations is 4 Hz, which is the highest frequency achieved or considered in the prototypes or studies presented, among others, by Eriksen et al. (2015), Jacobs et al. (2014), Tomc et al. (2014), Trevizoli and Barbosa (2015), Tura and Rowe (2011), Tušek et al. (2010), and Zimm et al. (2006). In the studies reported by Engelbrecht et al. (2012) and Lozano et al. (2014) higher frequencies are tried but the performance has not been better than what is achieved at 4 Hz or lower frequencies. In an early report on constructing a rotary magnetic refrigeration device, Buchelnikov et al. (2007) have mentioned that the rotary part of their device can rotate at speeds up to 10 Hz without publishing the results on the performance of the device with the test conditions. Although frequencies an order of magnitude higher than 4 Hz may (or may not) be viable in the future according to Kuz'min (2007), such frequencies are not considered since the focus of this work is on developing the materials not improving the design of the devices. In addition at higher frequencies friction losses in flow distribution system (e.g. rotary valve) and the moving part of the magnetic circuit becomes more important, but these losses are not included in the model.

The heat transfer fluid is aqueous ethanol solution. The concentration needed to prevent freezing is 25% by volume for all the simulations. The corrosion inhibitors, usually mixed with HTF in small concentrations, are assumed not affecting the thermophysical properties of HTF. In the magnetic refrigerators, the total efficiency of the motor and power transmission system driving the magnet assembly is assumed 90% and the total efficiency of the pump circulating HTF is assumed 70%. The porosity of the beds in the simulations is 0.36. The pressure drop outside the regenerators is neglected.

## 2.4 Simulation model and optimization process

The regenerators of the magnetic refrigeration systems are modeled using the 1-dimensional set of partial differential equations below, Eq. (4) (Engelbrecht 2008).

$$\begin{cases} -\rho_f V_D c_{p,f} \frac{\partial T_f}{\partial x} + k_{ef,f} \frac{\partial^2 T_f}{\partial x^2} - V_D \frac{\partial P}{\partial x} + h_{sf,corr} a (T_s - T_f) = \varepsilon \rho_f c_{p,f} \frac{\partial T_f}{\partial t} \\ k_{ef,s} \frac{\partial^2 T_s}{\partial x^2} + h_{sf,corr} a (T_f - T_s) - (1 - \varepsilon) \rho_s T_s \frac{\partial s}{\partial H} \frac{\partial H}{\partial t} = (1 - \varepsilon) \rho_s c_{H,s} \frac{\partial T_s}{\partial t} \end{cases} \quad (4)$$

The solid-fluid convective heat transfer coefficient, corrected for the internal conductive resistance of the solid phase in absence of any binding agent, is calculated using the Eqs. (5), suggested by Wakao and Kagueli (1982), and (6), suggested by Dixon and Cresswell (1979) and Nield and Bejan (2013). This heat transfer coefficient couples the equations for the fluid phase and the solid phase in Eq. (4).

$$h_{sf} = \frac{k_f}{d_p} \left( 2 + 1.1 Pr^{1/3} Re_d^{0.6} \right) \quad (5)$$

$$\frac{1}{h_{sf,corr}} = \frac{1}{h_{sf}} + \frac{d_p}{10k_s} \quad (6)$$

The effective thermal conductivities, considering dispersion effect, are given by Eqs. (7) and (8) for the fluid and solid phases (Amiri and Vafai 1998). For discussion about these equations and comparison to the similar equations used for the same purpose see the work by Monfared (2018b).

$$k_{ef,f} = k_f (\varepsilon + 0.5 Re_d Pr) \quad (7)$$

$$k_{ef,s} = (1 - \varepsilon) k_s \quad (8)$$

The pressure gradient is calculated using Eq. (9) (Macdonald et al. 1979).

$$-\frac{dP}{dx} = \frac{180(1-\varepsilon)^2 \mu_f}{d_p^2 \varepsilon^3} V_D + \frac{1.8 \rho_f (1-\varepsilon)}{d_p \varepsilon^3} V_D^2 \quad (9)$$

The heat exchangers are modeled using  $\varepsilon$ - $NTU$  method for cross-flow, air-liquid heat exchangers, as explained in details by Monfared (2018b). The model of the heat exchangers is coupled to the model of the regenerators. For example, the input temperature on the fluid side of the cold heat exchanger is equal to the fluid temperature leaving the cold end of the regenerators, and the temperature of the fluid entering the cold end of the regenerators is equal to the temperature of the liquid leaving the cold heat exchanger. The warm heat exchanger is coupled to the regenerators' model in a similar way. The air-side inlet temperatures of the heat exchangers are fed as constant inputs to the simulation model of the magnetic refrigeration system.

The cooling capacity and heating capacity are calculated by Eqs. (10) and (11). The pumping power is calculated by Eq. (12).

$$Q_C = \frac{Nr}{\tau} \left( \int^{V_D > 0} \dot{m}_f i_{C,R} dt - \int^{V_D < 0} |\dot{m}_f| i_{C,L} dt \right) \quad (10)$$

$$Q_H = \frac{Nr}{\tau} \left( \int^{V_D > 0} \dot{m}_f i_{H,L} dt - \int^{V_D < 0} |\dot{m}_f| i_{H,R} dt \right) \quad (11)$$

$$\dot{W}_{pump} = Nr \left( \int_0^L \int_0^\tau |V_D| A_c \left| \frac{dP}{dx} \right| dt dx \right) / \tau \quad (12)$$

The magnetic work is deduced from Eq. (13).

$$\dot{W}_m = Q_H - Q_C - \dot{W}_{pump} \quad (13)$$

$COP_{total}$  is calculated by Eq. (14) using the pump and magnet drive efficiencies given in section 2.3.

$$COP_{total} = \frac{Q_c}{\dot{W}_m/0.9 + \dot{W}_{pump}/0.7} \quad (14)$$

For more details of the simulation model and its validation see the complete description of the model presented by Monfared (2018a). However, note that in the present study:

- The external magnetic field is not considered and all of the calculations are done for the internal field, as explained in section 2.3.
- The parasitic heat flux to the regenerators is neglected (see section 2.3).
- The heat source and heat sink are modeled as heat exchangers with limited  $UA$  values as explained by Monfared (2018b).

Optimization of the parameters to maximize the cooling capacity or efficiency is done through iterative parametric studies. That is, one parameter is varied at a time and the new optimum found for this parameter is used in other studies in which other parameters vary. This process is repeated until none of the parametric studies suggest a new, better value as the optimum. The parameters varied during the optimization process are: flow rate of HTF, length of regenerator (determining ratio of length to cross sectional area) while the volume is fixed, diameter of particles, operation frequency, and deviation of the transition temperature of each layer from its average operating temperature.

The exergetic cooling power, which is referred to several times in this article, is calculated according to Eq. 15 (Rowe 2011).

$$Ex_Q = Q_c \left( \frac{T_{ambient}}{T_{cabinet}} - 1 \right) \quad (15)$$

## 2.5 Modeling MCM and altering the properties

$\text{La}(\text{Fe}, \text{Mn}, \text{Si})_{13}\text{H}_z$  is one of the most promising materials available today for room-temperature magnetic refrigeration because of its large  $\Delta S_m$  and negligible hysteresis (Gutfleisch et al. 2016, Morrison et al. 2012). The field-dependent properties of the magnetocaloric materials are modeled based on the measured properties of  $\text{LaFe}_{11.384}\text{Mn}_{0.356}\text{Si}_{1.26}\text{H}_{1.52}$  published by Morrison et al. (2012). As the properties given by Morrison et al. (2012) are reported for external magnetic fields, they are evaluated at the corresponding internal fields by taking the demagnetizing factor of the measurement sample and magnetization into account ( $H_{in} = H_{ex} - NM$ ). To facilitate modifying the properties to create materials giving better performance, variations of heat capacity with temperature are modeled as functions with the general form shown by Eq. 16.

$$c_H = a_1 e^{-\left(\frac{T-b_1}{c_1}\right)^2} + a_2 e^{-\left(\frac{T-b_2}{c_2}\right)^2} \quad (16)$$

The parameters  $a_1$ ,  $b_1$ ,  $c_1$ ,  $a_2$ ,  $b_2$ , and  $c_2$  are not constants, but, to include the dependency of heat capacity of MCM on magnetic field, they are polynomial functions of the magnetic field with the general forms given by Eq. 17 and Eq. 18. Please note that for each of the parameters  $a_1$  to  $c_2$  the values  $p_0$ ,  $p_1$ , and  $p_2$ , determined through curve fitting, are different.

$$a_1, b_1, a_2, \text{ or } b_2 = p_1 H_{in} + p_0 \quad (17)$$

$$c_1 \text{ or } c_2 = p_2 H_{in}^2 + p_1 H_{in} + p_0 \quad (18)$$

Using Eq. 19, entropy, and thereby  $ds/dH_{in}$ , can be derived from heat capacity curves (Pecharsky and Gschneidner Jr 1999).

$$ds = \frac{c_H}{T} dT \quad (19)$$

To have different transition temperatures at different positions along the regenerators, the temperature-dependent properties of MCM are shifted and heat capacity is adjusted, as explained by Monfared and Palm (2015) so that the thermodynamic relations between the properties hold after the shift.

Figure 2 shows entropy as a function of temperature at two internal fields of 0 (the upper curve) and 400 k A m<sup>-1</sup> (the lower curve) and magnetocaloric effect in terms of adiabatic temperature change,  $\Delta T_{ad}$ , and isothermal entropy change,  $\Delta s_m$ .

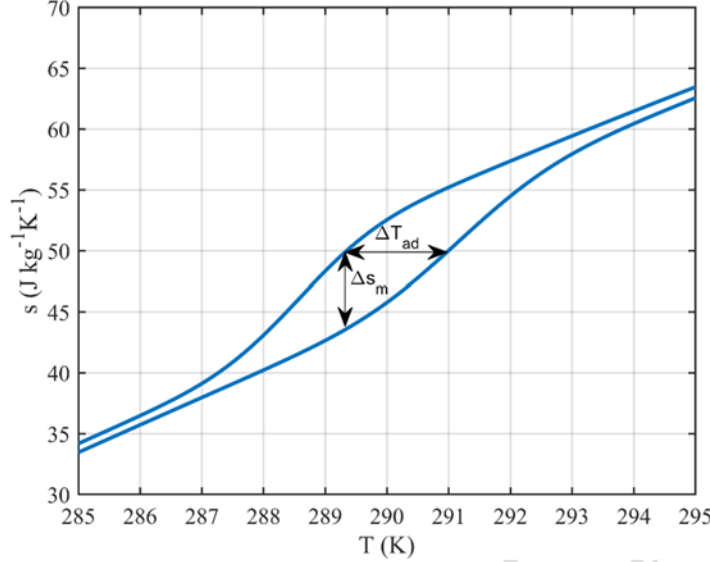


Figure 2: Entropy lines at 0 and 400 k A m<sup>-1</sup> internal field and magnetocaloric effect at an arbitrary point

Altering the magnetocaloric effect ( $\Delta s_m$  or  $\Delta T_{ad}$ ) is done mainly using the following two methods or their combination.

Method 1: To increase the isothermal entropy change,  $\Delta s_m$ , the slope of the curves in the vicinity of the transition temperature (where the two curves have larger distance) can be increased. It can be done by increasing either parameter  $a_1$  or  $a_2$  (while the coefficient to  $H_{in}$  in it is increased to a lesser extent). Two arbitrarily altered materials are shown in blue and red in addition to the base material shown in black in Figure 3. With this method, together with  $\Delta s_m$ , heat capacity has also changed considerably, which is not unexpected since entropy and heat capacity are related tightly according to Eq. 19. Therefore, some of the change in the performance of the magnetic refrigerator simulated with such altered  $\Delta s_m$  is due to the change in the heat capacity. Although increasing the  $\Delta T_{ad}$  is not the main purpose, it does not remain absolutely untouched with this method, but the change is not comparable to the increase in  $\Delta s_m$ . It should be noted that increasing the distance between the curves by simply shifting one of them vertically is not a proper solution since far from the transition temperature the two curves should get very close.

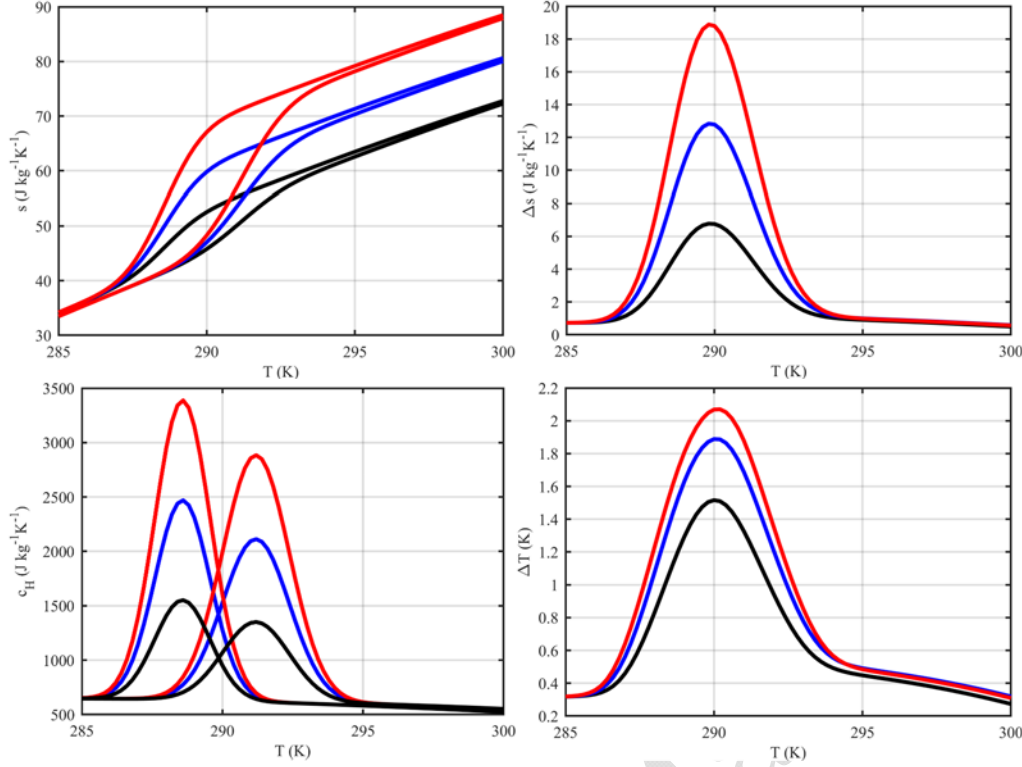


Figure 3: Altering materials to get higher  $\Delta s_m$ . The blue and red curves are for materials for which the  $c_H$  has been altered by modifying  $a_1$  or  $a_2$  in Eq. 16.

Method 2: To increase the  $\Delta T_{ad}$ , the horizontal distance shown in Figure 2 between the curves in the vicinity of the transition temperature should be increased while far from that temperature the curves related to different magnetic fields should remain close. To do that, the coefficient of  $H_{in}$  in either  $b_1$  or  $b_2$  can be altered. Figure 4 shows the results of such an alteration with the curves in black color showing the base material and the curves in blue and red for altered materials. Here, unlike for increasing  $\Delta s$ , the magnitude of the heat capacity remains virtually unchanged while the transition temperature becomes more sensitive to the magnetic field. That is,  $\Delta T_{ad}$  is increased by shifting the transition temperature of the materials further for the same change in the internal field, which is in accordance with what Pecharsky et al. (2001) have suggested. The unintended change in  $\Delta s$  is much smaller in this method compared to what is depicted in Figure 3 for Method 1.

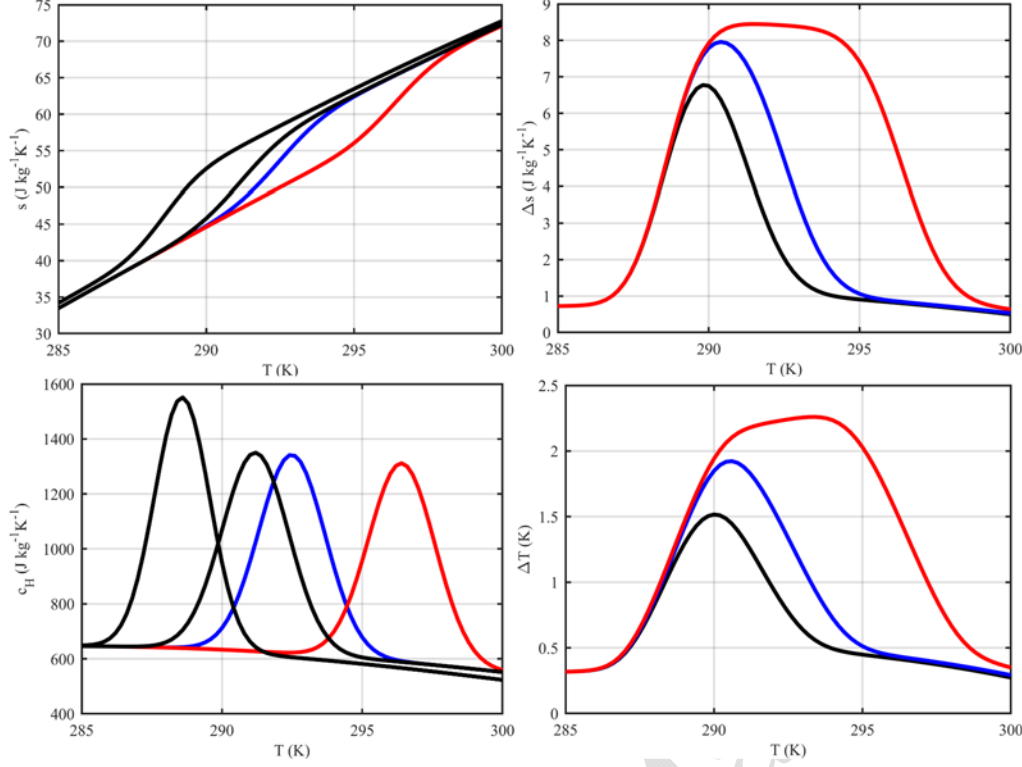


Figure 4: Altering materials to get higher  $\Delta T_{ad}$ . The blue and red curves are for materials for which the  $c_H$  has been altered by modifying  $b_1$  or  $b_2$  in Eq. 16. The leftmost  $c_H$  and  $s$  curves are common between the three materials when  $H_m=0$

The plateaus appearing in  $\Delta s_m$  and  $\Delta T_{ad}$  curves which are shown in red in Figure 4 are simply because of the shape of the  $s$  curves as their distance in the vicinity of the transition temperature remain almost constant when this distance becomes large.

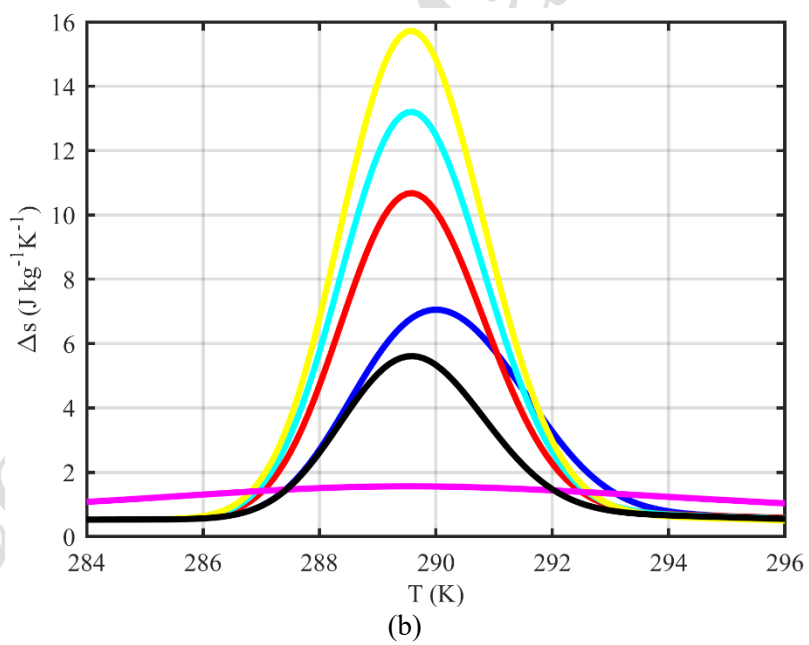
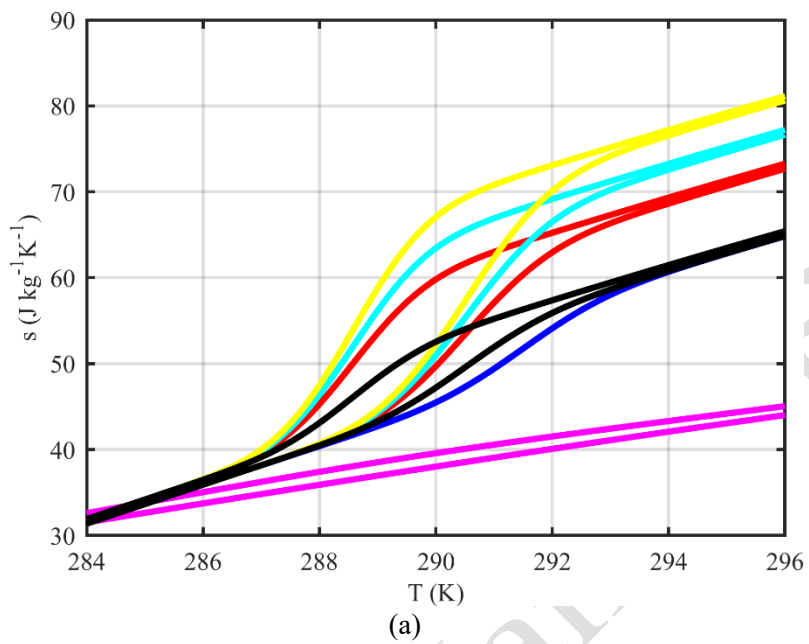
When simultaneous increase in magnetocaloric effect and decrease in heat capacity is desired, in addition to the above methods, parameters  $a_1$  and  $a_2$  are further manipulated.

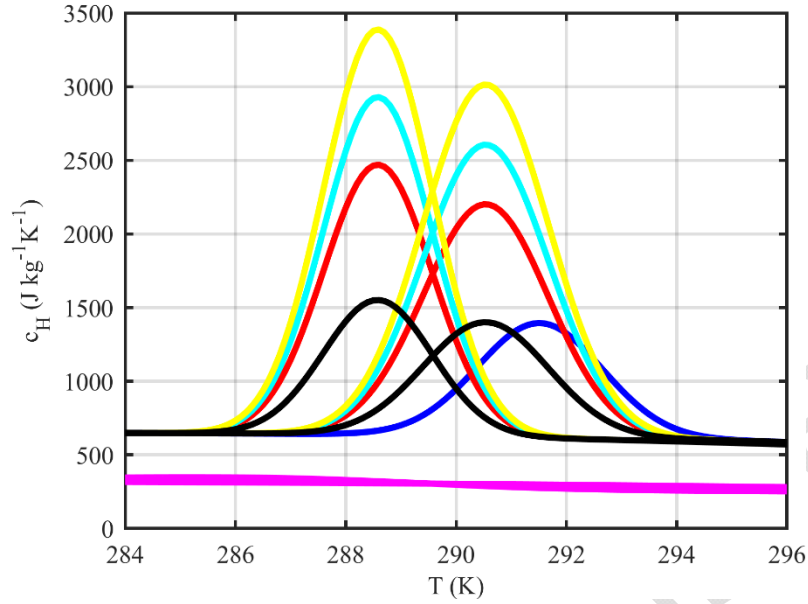
The altered materials used in this study are listed in Table 1 with their properties shown in Figure 5. The properties of gadolinium, as reported by Lozano et al. (2014), are also added to the list as a reference for comparison. The first material, mat<sub>1</sub>, which is also referred to as base material in the text, has the properties similar to the currently available  $\text{La}(\text{Fe},\text{Mn},\text{Si})_{13}\text{H}_z$  group of materials. The relative cooling power ( $RCP_s$ ) of each material is calculated using Eq. 20. This metric shows the potential of the materials well as single layers, while its calculation is simple (Niknia et al. 2017).  $FWHM_s$  is width of  $\Delta s_m$  curve versus temperature where  $\Delta s_m$  has half of its maximum value.

$$RCP_s = -\Delta s_{m,max} FWHM_s \quad (20)$$

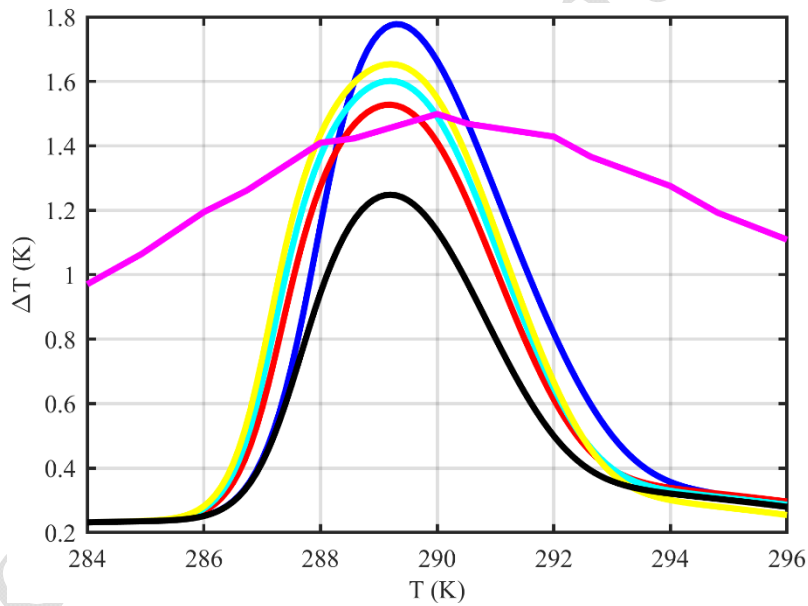
Table 1: List of materials the properties of which are shown in Figure 5. MCE and  $RCP_s$  are calculated for internal field change of 0 to 300 k A m<sup>-1</sup>

Material	Color	$RCP_s$	$\Delta T_{ad}$	$\Delta s_m$	$c_{H,max@0T}$
1	black	17.6	1.2	5.61	1550
2	blue	27.7	1.6	6.68	1550
3	red	32.0	1.5	10.7	2470
4	cyan	39.2	1.6	13.2	2930
5	yellow	46.4	1.7	15.7	3390





(c)



(d)

Figure 5: The materials used in the study shown in different colors according to Table 1.

The density of MCM is  $7100 \text{ kg m}^{-3}$  in the simulation model as given by Radulov et al. (2015). For thermal conductivity of MCM the constant value of  $8 \text{ W m}^{-1} \text{ K}^{-1}$  is used based on what is reported for similar materials by Fujieda et al. (2004) and Fukamichi et al. (2006).

## 2.6 Case 1

The first case is a display cabinet (professional refrigerated storage cabinet) with rather high cooling capacity compared to case 2 but lower efficiency. The performance of the display cabinet, cooled by a vapor-compression system, at two working conditions is summarized in Table 2. These data are provided by Electrolux AB.

Table 2: Performance of the display cabinet at two different working conditions (case 1)

	Moderate ambient	Warm ambient	Unit
$T_{cabinet}$	2	2	°C
$T_{ambient}$	25	43	°C
<b>cabinet load</b>	92	165	W
$Ex_Q$	10	28.8	W
Lights	28	28	W
<b>total load</b>	120	193	W
$P_{compressor}$	1.54	3.64	kWh (24h) <sup>-1</sup>
$P_{fans, evap \& cond}$	0.4	0.8	kWh (24h) <sup>-1</sup>
$P_{electric board \& light}$	0.68	0.68	kWh (24h) <sup>-1</sup>
$COP_{total}$	1.1	0.9	
$\eta_{Carnot}$	0.16	0.19	

As the lights are always on in the display cabinet, their power is added to the cooling load on the cabinet to calculate the total needed cooling capacity. It should be noted that the rather low energy efficiency rating of this refrigerator is partly due to the lights power consumption. The fan power of the evaporator is included in the cabinet load.

For the given data, the energy efficiency class for this display cabinet for the ambient temperature of 25 °C (climate class 3) is D with energy efficiency index (EEI) of 66.7, according to Commission Delegated Regulation (EU) 2015/1094 of 5 May 2015.

The same total cooling load and fan energy consumption over 24 hours is considered for the equivalent magnetic refrigeration system. However, since continuous operation, instead of the on-off cycles with vapor-compression system, is assumed for the magnetic refrigeration system, the air flow rate and UA-values of the heat exchangers are estimated as explained in section 2.3. Those estimated values are given in Table 3.

Table 3: Mass flow rate of air and UA-values for the heat exchangers of magnetic refrigerator at two working conditions (case 1)

	Moderate ambient	Warm ambient	Unit
$T_{cabinet}$	2	2	°C
$T_{ambient}$	25	43	°C
$P_{fan, evap}^a$	8	8	W
$P_{fan, cond}^a$	40	40	W
<b>run time</b> <sup>a</sup>	35	70	%
$UA_{evap}^a$ (running fan)	35	35	W K <sup>-1</sup>
$UA_{cond}^a$ (running fan)	27	27	W K <sup>-1</sup>
$UA_{CHX}$	26.4	31.8	W K <sup>-1</sup>
$UA_{HHX}$	20.3	24.5	W K <sup>-1</sup>
$\dot{m}_{air, CHX}$	0.035	0.044	kg s <sup>-1</sup>
$\dot{m}_{air, HHX}$	0.06	0.076	kg s <sup>-1</sup>

<sup>a</sup> For the corresponding vapor-compression refrigerator

## 2.7 Case 2

The second case is a household refrigerator with lower cooling load but higher efficiency. The performance of the refrigerator, cooled by a vapor-compression system, is summarized in Table 4. These data are provided by Electrolux. The fan power of the evaporator is included in the cabinet load.

Table 4: Performance of the vapor-compression household refrigerator (case 2)

		Unit
$T_{cabinet}$	5	°C
$T_{ambient}$	25	°C
cabinet load	29.1	W
$Ex_Q$	2.1	W
Lights	0	W
total load	29.1	W
$P_{compressor}$	0.17	kWh (24h) <sup>-1</sup>
$P_{fan, evap}$	0.013	kWh (24h) <sup>-1</sup>
$P_{electric board}$	0.017	kWh (24h) <sup>-1</sup>
$COP_{total}$	3.54	
$\eta_{Carnot}$	0.3	

For the given data, the energy efficiency class for this household refrigerator (temperate climate class) is A+++ with energy efficiency index (EEI) of 21.9, according to Commission Delegated Regulation (EU) 1060/2010 of 28 September 2010.

The same total cooling load and fan energy consumption over 24 hours is considered for the equivalent magnetic refrigeration system. However, since continuous operation, instead of the on-off cycles with vapor-compression system, is assumed for the magnetic refrigeration system, the air flow rate and  $UA$ -values of the cold heat exchanger are estimated as explained in section 2.3. Those estimated values are given in Table 5. The condenser, and accordingly the hot heat exchanger of the magnetic refrigeration system, are not equipped with fan.

Table 5: Mass flow rate of air and  $UA$ -values for the cold heat exchanger of magnetic refrigerator (case 2)

		Unit
$P_{fan, evap}$ <sup>a</sup>	1.3	W
run time <sup>a</sup>	41	%
$UA_{evap}$ <sup>a</sup> (running fan)	6	W K <sup>-1</sup>
$UA_{CHX}$	4.73	W K <sup>-1</sup>
$\dot{m}_{air, CHX}$	0.02	kg s <sup>-1</sup>

<sup>a</sup> The corresponding vapor-compression refrigerator

## 3 Results

### 3.1 Case 1

As the needed cooling capacity is rather high for case 1, the maximum volume of regenerators, 360 cm<sup>3</sup>, is used. The performance of the magnetic refrigeration system is evaluated for the two working conditions indicated in Table 2.

### 3.1.1 Ambient temperature of 25 °C

For the ambient temperature of 25 °C the base material,  $mat_1$ , satisfies the requirements for the performance of the magnetic refrigeration system to compete with the vapor-compression system. To provide at least 120 W cooling capacity with  $COP_{total}$  of 1.1 or more, the magnetic refrigeration system can be run with  $41.7 \text{ cm}^3 \text{ s}^{-1}$  maximum flow rate, 125  $\mu\text{m}$  particles, 0.04 m regenerator length, frequency of 4 Hz, and transition temperature of each layer 0.7 K higher than the average temperature of that layer during a cycle according to Figure 6, Figure 7, Figure 8, Figure 9, and Figure 10. These are the final results, showing the variation of one parameter while the rest are at their optimum values.

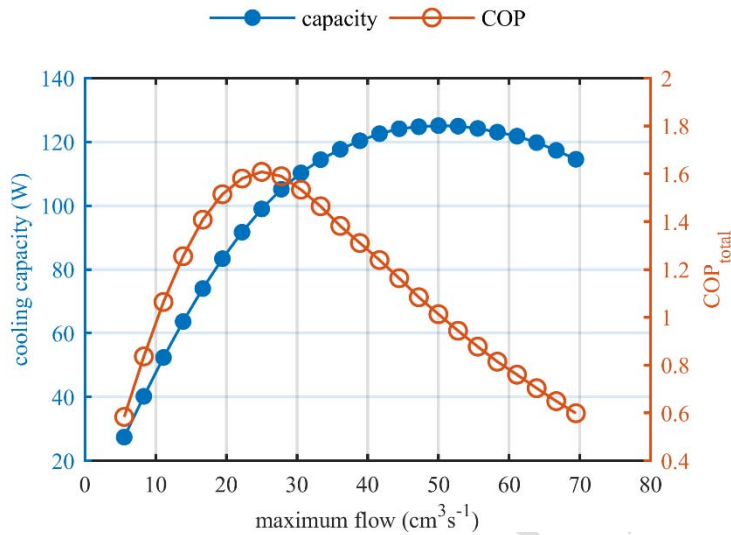


Figure 6: Effect of maximum flow rate on cooling capacity and  $COP_{total}$

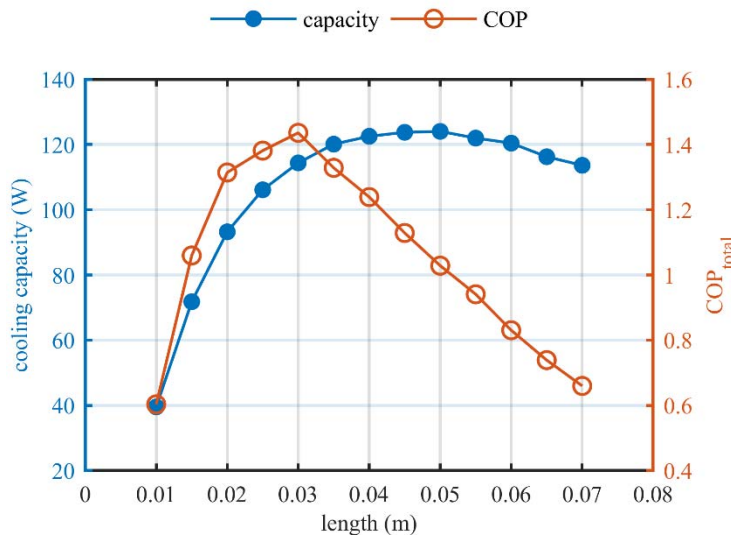


Figure 7: Effect of length of the regenerators (with constant total volume) on cooling capacity and  $COP_{total}$

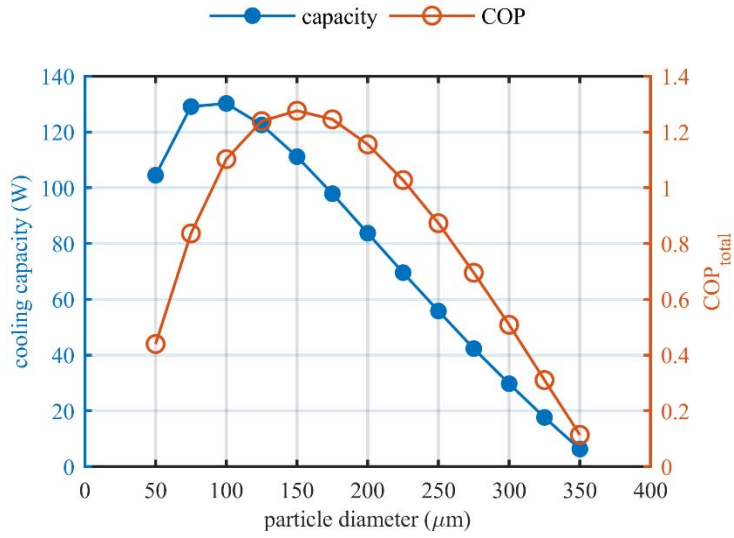


Figure 8: Effect of particle diameter on cooling capacity and  $COP_{total}$

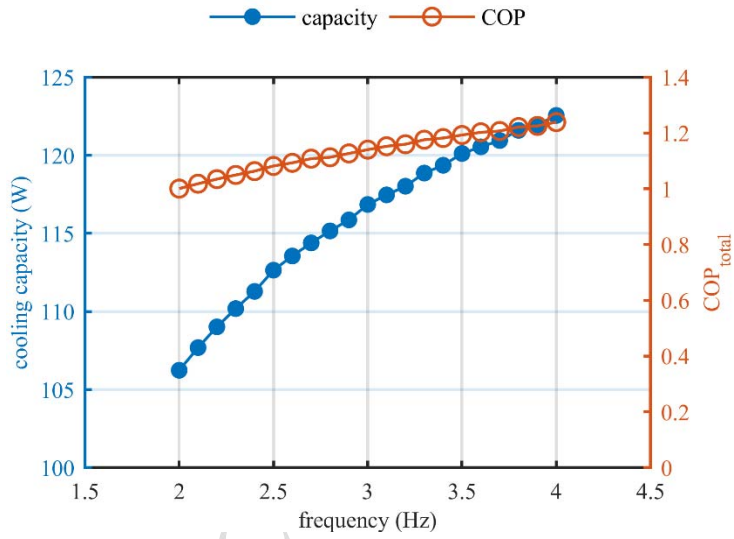


Figure 9: Effect of operation frequency on cooling capacity and  $COP_{total}$

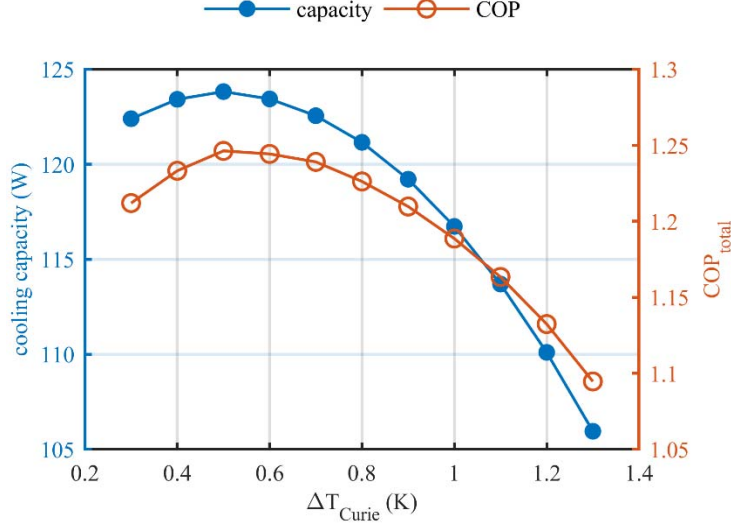


Figure 10: Effect of the choice of Curie temperature for each layer on cooling capacity and  $COP_{total}$

### 3.1.2 Ambient temperature of 43 °C

With ambient temperature of 43 °C the base material,  $mat_1$ , which has field-dependent properties similar to the currently available  $La(Fe,Mn,Si)_{13}H_z$  material, could not provide the required cooling capacity (193 W), while  $COP_{total}$  is over 0.9. Therefore, materials with enhanced properties, including  $mat_2$ ,  $mat_3$ , and  $mat_4$ , are tried. With  $mat_4$  the target performance is achieved and there is no need for further enhancement of the properties.

The magnetic refrigeration system with  $mat_4$ ,  $50 \text{ cm}^3 \text{ s}^{-1}$  maximum flow rate, 100  $\mu\text{m}$  particles, 0.06 m regenerator length, frequency of 4 Hz, and transition temperature of each layer 1 K higher than the average temperature of that layer during a cycle can provide 199 W cooling capacity with  $COP_{total}$  of 0.91. The highest cooling capacities with other materials and the corresponding  $COP_{total}$  for the conditions giving the highest cooling capacity are summarized in Table 6. The optimized performance for each material is calculated using a parametric study similar to what is presented in section 3.1.1.

Table 6: Performance of materials providing insufficient cooling capacity

Material	Highest cooling capacity (W)	$COP_{total}$
$mat_1$	106	0.60
$mat_2$	167	0.99
$mat_3$	182	0.79

## 3.2 Case 2

Compared to case 1, the temperature difference between the heat reservoirs and needed cooling capacity is smaller in case 2. Accordingly, the magnetic refrigeration system is expected to be more compact with less magnetocaloric material. For case 2 the total size of the regenerator is reduced proportional to the exergetic cooling power. If compared to case 1 with ambient temperature of 25 °C, the total volume of regenerators in case 2 becomes 75  $\text{cm}^3$ . If compared to case 1 with ambient temperature of 43 °C, the total volume of regenerators in case 2 becomes 26.2  $\text{cm}^3$ .

With 75 cm<sup>3</sup> total volume of the regenerators, mat<sub>1</sub>, can supply 30 W cooling capacity with  $COP_{total}$  of 4.32. The rest of the parameters are 8.3 cm<sup>3</sup> s<sup>-1</sup> maximum flow rate, 75 μm particles, 0.02 m regenerator length, frequency of 4 Hz, and transition temperature of each layer 0.3 K higher than the average temperature of that layer during a cycle. The particle diameter found through the optimization process is smaller than what is typically used in magnetic refrigeration prototypes. Since the smaller particle size increases the pressure drop per unit length, the optimum length of the regenerator is also short.

With 26.2 cm<sup>3</sup> total volume of the regenerators, the materials mat<sub>1</sub>, mat<sub>2</sub>, and mat<sub>3</sub> do not have the required properties to supply 29.1 W cooling capacity with  $COP_{total}$  of 3.54 or higher. However, with mat<sub>4</sub>, 5.6 cm<sup>3</sup> s<sup>-1</sup> maximum flow rate, 75 μm particles, 0.017 m regenerator length, frequency of 4 Hz, and transition temperature of each layer 0.3 K higher than the average temperature of that layer during a cycle,  $COP_{total}$  of 3.56 is achieved. By comparing  $\Delta S_m$ ,  $\Delta T_{ad}$ ,  $RCP_s$ , and  $c_H$  of the materials given in Table 1, it is observed that materials with higher  $\Delta S_m$  and lower  $c_H$  could help increasing  $COP_{total}$ . Therefore, the ratio of the maxima of these two parameters, a dimensionless number, is tabulated in Table 7 and  $COP_{total}$  is plotted against this ratio in Figure 11. Since mat<sub>1</sub> cannot supply the required cooling capacity, it is not included in Table 7 and Figure 11.

Table 7: Highest achieved  $COP_{total}$  for materials tried with 26.2 cm<sup>3</sup> total regenerator volume for case 2

Material	$\Delta S_{m,max}$	$c_{H,max@0field}$	$\Delta S_{m,max}/c_{H,max@0field}$	$RCP_s$	$\Delta S_{m,max}\Delta T_{ad,max}$	Highest $COP_{total}$
mat <sub>2</sub>	6.68	1550	0.0043	27.7	10.7	1.63
mat <sub>3</sub>	10.7	2470	0.0043	32.0	16.1	1.90
mat <sub>4</sub>	13.2	2930	0.0045	39.2	21.1	3.56
mat <sub>5</sub>	18.9	3390	0.0056	46.4	26.7	4.62

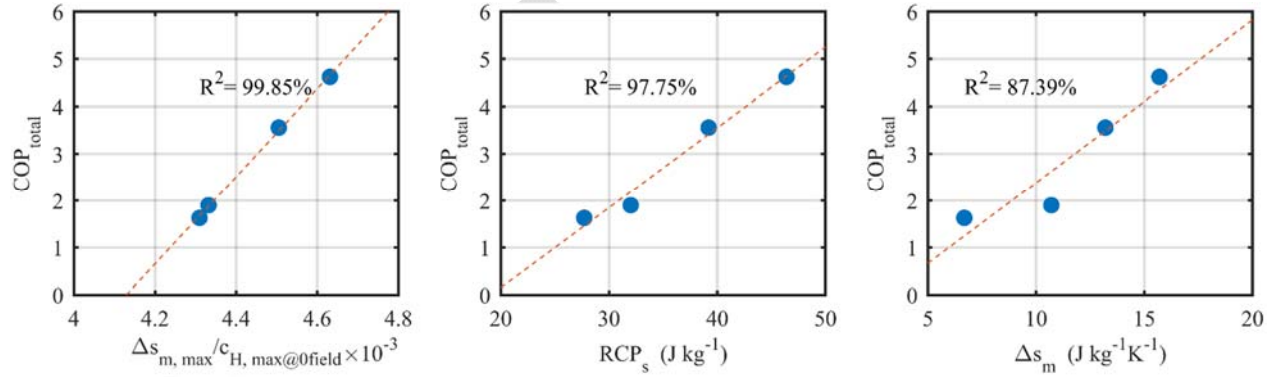


Figure 11:  $COP_{total}$  versus the ratio of the maxima of  $\Delta S_m$  and  $c_H$ ,  $RCP_s$ , and  $\Delta S_m$  for materials tried with 26.2 cm<sup>3</sup> total regenerator volume for case 2

As shown in Figure 11,  $COP_{total}$  increases with the ratio of the maxima of  $\Delta S_m$  and  $c_H$  linearly in the range where properties of the studied materials lie. To see if the linear trend holds for a material with higher ratio of the maxima of  $\Delta S_m$  and  $c_H$ , mat<sub>5</sub> is also tried. Smaller  $c_H$  value can be associated with larger adiabatic temperature change; however,  $c_H$  is not the only factor determining the magnitude of adiabatic temperature change (Pecharsky and Gschneidner Jr 1999). Therefore, such a linear relationship is not observed between the product of  $\Delta S_m$  and  $\Delta T_{ad}$  and  $COP_{total}$ . Two other parameters<sup>1</sup> showing linear relation with  $COP_{total}$  within

<sup>1</sup> In another study reported by Monfared (2018b), where a different system is investigated with wider range of materials, only the ratio of the maxima of  $\Delta S_m$  and  $c_H$  showed a linear relationship with  $COP_{total}$  not the two parameters  $RCP_s$  and  $\Delta S_m$ .

the range of the material properties tried in this study, although with less precision compared to the ratio of the maxima of  $\Delta S_m$  and  $c_H$ , are  $RCP_s$  and  $\Delta S_m$ . The lack of increasing, linear relationship between  $\Delta T_{ad}$  and  $COP_{total}$  in this study should not be interpreted as unimportance of  $\Delta T_{ad}$ , since with too low  $\Delta T_{ad}$  there is not enough driving force for heat transfer between the solid and fluid in the regenerator.

To examine whether the ratio of the maxima of  $\Delta S_m$  and  $c_H$ ,  $RCP_s$  and  $\Delta S_m$  are helpful in predicting the performance when the family of materials modeled in this study are compared with a different family of materials, case 2 with 26.2 cm<sup>3</sup> total volume of the regenerators is simulated with gadolinium and its alloys as MCM. The alloys of gadolinium with different phase transition temperatures are modeled as explained by Monfared and Palm (2015). With gadolinium and its alloys neither the ratio of the maxima of  $\Delta S_m$  and  $c_H$  nor  $RCP_s$  proved helpful, since their values for gadolinium, 0.0056 and 43.1 J kg<sup>-1</sup>, are comparable to those of the materials in Table 7, but the maximum obtained cooling capacity of 12.8 W (with  $COP_{total}$  of 0.74) is lower than the required capacity of case 2 fulfilled by the materials listed in that table. Accordingly, only  $\Delta S_m$ , at least qualitatively, can be helpful when two family of materials are compared in layered beds with enough number of layers to diminish the importance of the width of the peak in  $\Delta S_m$  as a function of temperature.

As an alternative to improving the materials, the performance can be enhanced by increasing the strength of the magnetic field. By using the base material which has the field-dependent properties of La(Fe,Mn,Si)<sub>13</sub>H<sub>z</sub> alloys and the maximum magnetic fields 2 and 2.5 times larger than what is indicated in Figure 1, the study is repeated for case 2. The highest obtained  $COP_{total}$  with those fields are 2.66 and 3.66. Thus, 2.5 times larger magnetic field change is needed to get the desired performance using the base material. However, to get that much increase in the maximum magnetic field, the needed mass of magnet material should be increased even more than 2.5 times (Bjørk et al. 2010). Therefore, considering that the mass of magnet decisively affects the price and the environmental impacts of magnet refrigeration, enhancing the performance through increasing the magnetic field is not a comprehensive solution (Bjørk et al. 2011, Monfared et al. 2014, Rowe 2009). In addition, the increased mass of magnet makes the magnetic refrigeration systems extra bulky and less fit for installation in the devices.

## 4 Discussion and conclusions

In this study it is investigated how much the properties of magnetocaloric materials need to be improved so that magnetic refrigeration systems can outperform vapor compression ones. Some of these properties are not a part of the simulation model, which is used as a tool in the study. However, the importance of improvement in those properties should not be overlooked. For example, the mechanical strength of the materials should be high enough so that the particles do not pulverize during magnetization cycles; otherwise, binding agents such as epoxy are needed, which lower the performance as discussed by Monfared (2018a). The properties to be improved but not included in the parametric studies are: uniform transitions temperature for each layer, 1 K increment in transition temperature in adjacent layers, and mechanical strength of the materials. Throughout the study, it is assumed that these requirements are met.

With the currently existing materials, the simulated magnetic refrigeration system could show a performance better than that of an actual, commercial class D vapor-compression system with low  $COP_{total}$ , moderate temperature span and moderate cooling capacity (case 1 with ambient temperature of 25 °C). However, to compete with a vapor-compression cycle with rather large cooling capacity, large temperature span, and still low  $COP_{total}$  the field-dependent properties of MCM layers need to be improved (e.g. 2.35 times larger  $\Delta S_m$  in mat<sub>4</sub> compared to the base material in case 1 with ambient temperature of 43 °C). As explained in Section 2.3, maximum allowed MCM is limited in this study to have reasonably sized magnetic

refrigeration system; otherwise, the deficit in cooling capacity when the base material is used can be compensated by enlarging the system.

For the case 2 in which the existing vapor-compression system has high  $COP_{total}$  ( $=3.54$ ), which is a class A+++ household refrigerator, similar comparison to simulated performance of magnetic refrigerator is done. In case 2, the required cooling capacity of the refrigerator is much lower compared to case 1; therefore, a more compact cooling system with less magnetic materials is expected. The amount of materials, in addition to the cost and environmental impacts (Bjørk et al. 2011, Monfared et al. 2014, Rowe 2009), affect the maximum obtainable efficiency although it is not immediately obvious. With extravagantly large total regenerator volume (which implies large magnet assembly) there is more room to optimize the parameters to increase COP with poor cooling power per unit volume; however, this solution is impractical as the cost and environmental impacts become large. Accordingly, the amount of MCM is reduced in case 2 (compared to case 1) proportional to the required exergetic cooling power. If the volume of case 2 is decided based on case 1 running at a moderate ambient temperature of  $25\text{ }^{\circ}\text{C}$  (which is not the ultimate working conditions for which case 1 is designed), the base material can give better performance than what is obtained from the vapor-compression system. However, with stricter limit on volume, based on the required exergetic cooling power in case 2 and that of case 1 when run at  $43\text{ }^{\circ}\text{C}$  ambient temperature, mat1, mat2, and mat3 fail to give the required  $COP_{total}$ , while mat4 satisfies the requirements for case 2. Compared to the base material, mat4 has 2.35 times higher  $\Delta S_m$ , 1.24 times higher ratio of the maxima of  $\Delta S_m$  and  $c_H$ , and 2.2 time higher  $RCP_s$ .

For both cases 1 with demanding conditions and case 2 with reduced volume of regenerators proportional to the needed exergetic cooling power, the same material,  $mat_4$ , gave the desired performance. With increased cooling demand, the same magnetocaloric material in magnetic refrigerators can give the same level of performance as long as the volume of the regenerators are varied proportional to the required exergetic cooling power. However, if the working temperatures vary drastically from one magnetic refrigerator to the other, the requirements for the magnetocaloric materials used in the refrigerator with lower level of operating temperatures are higher due to the increased viscosity of HTF, which leads to escalated viscous dissipation and pumping power. In case the working temperatures of the HTF drops below the freezing point of water, e.g. in refrigerator-freezers, the requirements for the materials become even more demanding since the needed anti-freeze in the HTF increases the viscosity considerably.

For the materials capable of producing enough cooling capacity for case 2, listed in Table 7, it is observed that  $COP_{total}$  has linear relation with the ratio of the maxima of  $\Delta S_m$  and  $c_H$ , and with lesser precision, with  $RCP_s$  and  $\Delta S_m$ . However, the ratio of the maxima of  $\Delta S_m$  and  $c_H$  and  $RCP_s$  turned out less meaningful when the materials in Table 7 are compared with another family of materials, Gd and its alloys. Thus, for comparing different family of materials in multi-layered regenerators the factor  $\Delta S_m$  seem to be a better metric for performance of the magnetocaloric materials.

By employing large volume of the regenerators or increased field intensity, the parameters can be chosen with less constraints to maximize  $COP_{total}$ , while the low power density of the device is compensated by the high field intensity or large volume of the regenerators. Nevertheless, such solutions are not desirable as they result in larger physical dimensions of the refrigeration system, while usually the available space is limited in practice. Moreover, larger amount of magnet material, either because of larger volume of regenerators or because of the need for higher magnetic field, adds to the costs and environmental impacts of magnetic refrigeration systems significantly.

The requirements for the materials indicated in this study are for the applications called case 1 and case 2 with the limits and assumptions explained. It is possible that the requirements for the materials be different

in other applications. In addition, the suggested improvements in the material properties do not substantiate the claim that such materials with improved properties are necessarily possible to make.

## Acknowledgments

We would gratefully like to acknowledge that this study was financed by the Swedish Energy Agency, grant number 40330-1, and Electrolux through the research program EFFSYS EXPAND. We would also like to thank Dr. Richard Furberg from Electrolux for sharing technical information about existing vapor-compression refrigeration systems. The computations were performed on resources provided by the Swedish National Infrastructure for Computing (SNIC) at PDC Centre for High Performance Computing (PDC-HPC).

## References

- Amiri, A., and K. Vafai. 1998. "Transient analysis of incompressible flow through a packed bed." *International Journal of Heat and Mass Transfer* 41 (24):4259-4279. doi: 10.1016/S0017-9310(98)00120-3.
- Balli, M., S. Jandl, P. Fournier, and A. Kedous-Lebouc. 2017. "Advanced materials for magnetic cooling: Fundamentals and practical aspects." *Applied Physics Reviews* 4 (2):021305. doi: 10.1063/1.4983612.
- Bjørk, R., C. R. H. Bahl, and K. K. Nielsen. 2016. "The lifetime cost of a magnetic refrigerator." *International Journal of Refrigeration* 63:48-62. doi: 10.1016/j.ijrefrig.2015.08.022.
- Bjørk, R., C. R. H. Bahl, A. Smith, and N. Pryds. 2010. "Review and comparison of magnet designs for magnetic refrigeration." *International Journal of Refrigeration* 33 (3):437-448. doi: 10.1016/j.ijrefrig.2009.12.012.
- Bjørk, R., A. Smith, C. R. H. Bahl, and N. Pryds. 2011. "Determining the minimum mass and cost of a magnetic refrigerator." *International Journal of Refrigeration* 34 (8):1805-1816. doi: 10.1016/j.ijrefrig.2011.05.021.
- Brown, G. V. 1976. "Magnetic heat pumping near room temperature." *Journal of Applied Physics* 47 (8):3673-3680. doi: 10.1063/1.323176.
- Brück, E., O. Tegus, D. T. Cam Thanh, N. T. Trung, and K. H. J. Buschow. 2008. "A review on Mn based materials for magnetic refrigeration: Structure and properties." *International Journal of Refrigeration* 31 (5):763-770. doi: 10.1016/j.ijrefrig.2007.11.013.
- Buchelnikov, V. D., S. V. Taskaev, I. V. Bychkov, I. A. Chernets, and A. N. Denisovskiy. 2007. "The prototype of effective device for magnetic refrigeration." Second IIF-IIR International Conference on Magnetic Refrigeration at Room Temperature, Portoroz, Slovenia.
- Dixon, A. G., and D. L. Cresswell. 1979. "Theoretical prediction of effective heat transfer parameters in packed beds." *AIChE Journal* 25 (4):663-676. doi: 10.1002/aic.690250413.
- Dung, N.H., Z.Q. Ou, L. Caron, L. Zhang, D.T.C. Thanh, G.A. Wijs, R.A. Groot, K.H.J. Buschow, and E. Bruck. 2011. "Mixed magnetism for refrigeration and energy conversion." *Advanced Energy Materials* 1 (6):1215-1219. doi: 10.1002/aenm.201100252.
- Engelbrecht, K., D. Eriksen, C. R. H. Bahl, R. Bjørk, J. Geyti, J. A. Lozano, K. K. Nielsen, F. Saxild, A. Smith, and N. Pryds. 2012. "Experimental results for a novel rotary active magnetic regenerator." *International Journal of Refrigeration* 35 (6):1498-1505. doi: 10.1016/j.ijrefrig.2012.05.003.
- Engelbrecht, Kurt. 2008. "A Numerical Model of an Active Magnetic Regenerator Refrigerator with Experimental Validation." PhD, Mechanical Engineering, University of Wisconsin-Madison.
- Eriksen, D., K. Engelbrecht, C. R. H. Bahl, R. Bjørk, K. K. Nielsen, A. R. Insinga, and N. Pryds. 2015. "Design and experimental tests of a rotary active magnetic regenerator prototype." *International Journal of Refrigeration* 58:14-21. doi: 10.1016/j.ijrefrig.2015.05.004.

- Franco, V., J. S. Blázquez, B. Ingale, and A. Conde. 2012. "The Magnetocaloric Effect and Magnetic Refrigeration Near Room Temperature: Materials and Models." *Annual Review of Materials Research* 42 (1):305-342. doi: 10.1146/annurev-matsci-062910-100356.
- Fujieda, S., Y. Hasegawa, A. Fujita, and K. Fukamichi. 2004. "Thermal transport properties of magnetic refrigerants  $\text{La}(\text{Fe}_x\text{Si}_{1-x})_{13}$  and their hydrides, and  $\text{Gd}_5\text{Si}_2\text{Ge}_2$  and  $\text{MnAs}$ ." *Journal of Applied Physics* 95 (5):2429-2431. doi: 10.1063/1.1643774.
- Fukamichi, K., A. Fujita, and S. Fujieda. 2006. "Large magnetocaloric effects and thermal transport properties of  $\text{La}(\text{FeSi})_{13}$  and their hydrides." *Journal of Alloys and Compounds* 408-412:307-312. doi: 10.1016/j.jallcom.2005.04.022.
- Gutfleisch, O., T. Gottschall, M. Fries, D. Benke, I. Radulov, K. P. Skokov, H. Wende, M. Gruner, M. Acet, P. Entel, and M. Farle. 2016. "Mastering hysteresis in magnetocaloric materials." *Philosophical Transactions of the Royal Society A: Mathematical, Physical and Engineering Sciences* 374 (2074). doi: 10.1098/rsta.2015.0308.
- Gutfleisch, Oliver, Matthew A. Willard, Ekkes Brück, Christina H. Chen, S. G. Sankar, and J. Ping Liu. 2011. "Magnetic Materials and Devices for the 21st Century: Stronger, Lighter, and More Energy Efficient." *Advanced Materials* 23 (7):821-842. doi: 10.1002/adma.201002180.
- Jacobs, S., J. Auringer, A. Boeder, J. Chell, L. Komorowski, J. Leonard, S. Russek, and C. Zimm. 2014. "The performance of a large-scale rotary magnetic refrigerator." *International Journal of Refrigeration* 37 (0):84-91. doi: 10.1016/j.ijrefrig.2013.09.025.
- Kitanovski, Andrej, Jaka Tušek, Urban Tomc, Uroš Plaznik, Marko Ožbolt, and Alojz Poredoš. 2015. *Magnetocaloric Energy Conversion: From Theory to Applications, Green Energy and Technology*: Springer.
- Kuz'min, M. D. 2007. "Factors limiting the operation frequency of magnetic refrigerators." *Applied Physics Letters* 90 (25):251916-3.
- Lei, Tian, Kurt Engelbrecht, Kaspar K. Nielsen, and Christian T. Veje. 2017. "Study of geometries of active magnetic regenerators for room temperature magnetocaloric refrigeration." *Applied Thermal Engineering* 111:1232-1243. doi: 10.1016/j.applthermaleng.2015.11.113.
- Lei, Tian, Kaspar K. Nielsen, Kurt Engelbrecht, Christian R. H. Bahl, Henrique Neves Bez, and Christian T. Veje. 2015. "Sensitivity study of multi-layer active magnetic regenerators using first order magnetocaloric material  $\text{La}(\text{Fe,Mn,Si})_{13}\text{Hy}$ ." *Journal of Applied Physics* 118 (1):014903. doi: 10.1063/1.4923356.
- Lozano, J. A., K. Engelbrecht, C. R. H. Bahl, K. K. Nielsen, J. R. Barbosa Jr, A. T. Prata, and N. Pryds. 2014. "Experimental and numerical results of a high frequency rotating active magnetic refrigerator." *International Journal of Refrigeration* 37 (0):92-98. doi: 10.1016/j.ijrefrig.2013.09.002.
- Macdonald, I. F., M. S. El-Sayed, K. Mow, and F. A. L. Dullien. 1979. "Flow through Porous Media-the Ergun Equation Revisited." *Industrial & Engineering Chemistry Fundamentals* 18 (3):199-208. doi: 10.1021/i160071a001.
- Monfared, Behzad. 2018a. "Design and optimization of regenerators of a rotary magnetic refrigeration device using a detailed simulation model." doi: 10.1016/j.ijrefrig.2018.01.011.
- Monfared, Behzad. 2018b. "Magnetic Refrigeration for Near Room-Temperature Applications." Doctoral thesis, Department of Energy Technology, KTH Royal Institute of Technology.
- Monfared, Behzad, Richard Furberg, and Björn Palm. 2014. "Magnetic vs. vapor-compression household refrigerators: A preliminary comparative life cycle assessment." *International Journal of Refrigeration* 42 (0):69-76. doi: 10.1016/j.ijrefrig.2014.02.013.
- Monfared, Behzad, and Björn Palm. 2015. "Optimization of layered regenerator of a magnetic refrigeration device." *International Journal of Refrigeration* 57:103-111. doi: 10.1016/j.ijrefrig.2015.04.019.
- Monfared, Behzad, and Björn Palm. 2016. "New magnetic refrigeration prototype with application in household and professional refrigerators." 7th International Conference on Magnetic Refrigeration at Room Temperature, Thermag VII, Turin.

- Morrison, K., K. G. Sandeman, L. F. Cohen, C. P. Sasso, V. Basso, A. Barcza, M. Katter, J. D. Moore, K. P. Skokov, and O. Gutfleisch. 2012. "Evaluation of the reliability of the measurement of key magnetocaloric properties: A round robin study of La(Fe,Si,Mn)H<sub>8</sub> conducted by the SSEEC consortium of European laboratories." *International Journal of Refrigeration* 35 (6):1528-1536. doi: 10.1016/j.ijrefrig.2012.04.001.
- Neves Bez, Henrique, Kristina Navickaitė, Tian Lei, Kurt Engelbrecht, Alexander Barcza, and Christian Bahl. 2016. "Epoxy-bonded La(Fe,mn,si)<sub>13</sub>H<sub>2</sub> As A Multi Layered Active Magnetic Regenerator." the 7th International Conference on Magnetic Refrigeration at Room Temperature, Turin.
- Nield, Donald A., and Adrian Bejan. 2013. *Convection in Porous Media*. New York, NY: Springer New York.
- Nielsen, K. K., C. R. H. Bahl, A. Smith, K. Engelbrecht, U. L. Olsen, and N. Pryds. 2014. "The influence of non-magnetocaloric properties on the performance in parallel-plate AMRs." *International Journal of Refrigeration* 37:127-134. doi: 10.1016/j.ijrefrig.2013.09.022.
- Nielsen, K. K., J. Tusek, K. Engelbrecht, S. Schopfer, A. Kitanovski, C. R. H. Bahl, A. Smith, N. Pryds, and A. Poredos. 2011. "Review on numerical modeling of active magnetic regenerators for room temperature applications." *International Journal of Refrigeration* 34 (3):603-616. doi: 10.1016/j.ijrefrig.2010.12.026.
- Niknia, I., P. V. Trevizoli, T. V. Christiaanse, P. Govindappa, R. Teyber, and A. Rowe. 2017. "Material screening metrics and optimal performance of an active magnetic regenerator." *Journal of Applied Physics* 121 (6):064902. doi: 10.1063/1.4975833.
- Pecharsky, V. K., and K. A. Gschneidner Jr. 1999. "Magnetocaloric effect from indirect measurements: Magnetization and heat capacity." *Journal of Applied Physics* 86 (1):565-575.
- Pecharsky, V. K., K. A. Gschneidner, A. O. Pecharsky, and A. M. Tishin. 2001. "Thermodynamics of the magnetocaloric effect." *Physical Review B* 64 (14):144406.
- Radulov, Iliya A., Konstantin P. Skokov, Dmitriy Yu Karpenkov, Tino Gottschall, and Oliver Gutfleisch. 2015. "On the preparation of La(Fe,Mn,Si)<sub>13</sub>H<sub>x</sub> polymer-composites with optimized magnetocaloric properties." *Journal of Magnetism and Magnetic Materials* 396:228-236. doi: 10.1016/j.jmmm.2015.08.044.
- Rowe, A. 2009. "Performance Metrics for Active Magnetic Refrigerators." 3rd IIF-IIR Conference on Magnetic Refrigeration at Room Temperature, Iowa, USA.
- Rowe, A. 2011. "Configuration and performance analysis of magnetic refrigerators." *International Journal of Refrigeration* 34 (1):168-177. doi: 10.1016/j.ijrefrig.2010.08.014.
- Tomc, Urban, Jaka Tušek, Andrej Kitanovski, and Alojz Poredoš. 2014. "A numerical comparison of a parallel-plate AMR and a magnetocaloric device with embodied micro thermoelectric thermal diodes." *International Journal of Refrigeration* 37:185-193. doi: 10.1016/j.ijrefrig.2013.07.003.
- Trevizoli, Paulo V., and Jader R. Barbosa Jr. 2015. "Entropy Generation Minimization analysis of oscillating-flow regenerators." *International Journal of Heat and Mass Transfer* 87:347-358. doi: 10.1016/j.ijheatmasstransfer.2015.03.079.
- Tura, A., and A. Rowe. 2011. "Permanent magnet magnetic refrigerator design and experimental characterization." *International Journal of Refrigeration* 34 (3):628-639. doi: 10.1016/j.ijrefrig.2010.12.009.
- Tušek, J., S. Zupan, A. Šarlah, I. Prebil, and A. Poredoš. 2010. "Development of a rotary magnetic refrigerator." *International Journal of Refrigeration* 33 (2):294-300. doi: 10.1016/j.ijrefrig.2009.11.003.
- Tušek, Jaka, Andrej Kitanovski, Urban Tomc, Chiara Favero, and Alojz Poredoš. 2014. "Experimental comparison of multi-layered La-Fe-Co-Si and single-layered Gd active magnetic regenerators for use in a room-temperature magnetic refrigerator." *International Journal of Refrigeration* 37 (0):117-126. doi: 10.1016/j.ijrefrig.2013.09.003.
- Wakao, Noriaki, and S Kagueli. 1982. *Heat and Mass Transfer in Packed Beds*. Edited by R Hughes, *Topics in Chemical Engineering*. New York: Gordon and Breach, Science Publishers, Inc.

Zimm, C., A. Boeder, J. Chell, A. Sternberg, A. Fujita, S. Fujieda, and K. Fukamichi. 2006. "Design and performance of a permanent-magnet rotary refrigerator." *International Journal of Refrigeration* 29 (8):1302-1306. doi: 10.1016/j.ijrefrig.2006.07.014.

Accepted Manuscript